

Redox-Active, Multinuclear (Ferrocenylethynyl)phosphanes and Their Palladium and Platinum Complexes

Thomas Baumgartner,^{*,†,‡} Marcel Fiege,[‡] Florian Pontzen,[‡] and Rocio Arteaga-Müller[‡]

Department of Chemistry, University of Calgary, 2500 University Drive NW, Calgary, AB, T2N 1N4, Canada, and Institute of Inorganic Chemistry, RWTH-Aachen University, Landoltweg 1, 52074 Aachen, Germany

Received July 31, 2006

A series of (ferrocenylethynyl)phosphanes with increasing number of ferrocenylethynyl units, including corresponding PdCl₂, PtCl₂, and PdI₂ complexes were prepared, their spectroscopic data investigated, and the solid-state structures of three of the complexes determined. The complexes exhibit increased steric bulk, affording bent ethynyl moieties in the *cis*-configured PdCl₂ and PtCl₂ complex. The PdI₂-based complex shows a favorable *trans*-configuration with almost linear acetylene units. The thermal behavior of some of the complexes indicated their utility as potential precursors for magnetic ceramic nanomaterials. Electrochemical investigations of the ligands and the corresponding complexes revealed that the structural motif of the ligands does not support multistep redox processes within the materials. All compounds showed single, reversible redox processes whose potential is influenced by the substitution pattern of the ligands as well as the respective complex geometries.

Introduction

The incorporation of metal atoms into supramolecular assemblies and macromolecules is an intriguing perspective for the development of new materials with novel, unusual properties.¹ Transition metal centers can, for example, permit redox control of the size and shape of a macroscopic object,² selective binding and sensing,³ the generation of liquid crystalline materials⁴ or magnetic nanoparticle composites,^{5,6} and etch resistance to plasmas,⁷ as well as several other useful physical and chemical characteristics.⁸ With regard to molecular electronics, these features have become particularly desirable in recent years, and

highly metallized, molecular materials are thus exciting research targets.^{1,9} Main chain metallopolymers with covalent bonds are now relatively well developed, as nicely illustrated by systems such as polyferrocenes and polymetallaynes.^{1,10} The use of coordinate bonds for the construction of highly metallized macromolecular and supramolecular materials, however, provides an attractive alternative approach.^{11,12} Most work in this area to date has focused on the use of bidentate, nitrogen-donor ligands, and building blocks employed as spacers in these ligands almost exclusively rely on π -conjugated units such as arylenes, arylene-vinylenes, or nonconjugated oligo(ethylene-glycol)s.¹³ The use of value-added, "smart" linkers that incorporate additional redox or optical features, on the other hand, is surprisingly rare; only a few reports in the literature utilize, for example, ferrocene units as an integral part of the spacer ligands, despite its highly valuable redox properties, chemical robustness, and versatility.¹⁴ It is also striking that, although phosphane ligation is ubiquitous in molecular transition metal

* Author to whom correspondence should be addressed. E-mail: thomas.baumgartner@ucalgary.ca.

[†] Current address: University of Calgary.

[‡] RWTH-Aachen University.

(1) (a) Archer, R. D. *Inorganic and Organometallic Polymers*; John Wiley & Sons Inc.: New York, 2001. (b) Manners, I. *Synthetic Metal Containing Polymers*; Wiley-VCH: Weinheim, 2004. (c) *Macromolecules Containing Metal and Metal-Like Elements*; Abd-el-Aziz, A. S., Carraher, C. E., Jr.; Pittman, C. U., Jr.; Sheats, J. E.; Zeldin, M., Eds.; Wiley: New York, 2004–2006; Vols. 1–7.

(2) (a) Yoshida, R.; Takahashi, T.; Yamaguchi, T.; Ichijo, H. *Adv. Mater.* **1997**, *9*, 175. (b) Arsenault, A. C.; Miguez, H.; Kitaev, V.; Ozin, G. A.; Manners, I. *Adv. Mater.* **2003**, *15*, 503.

(3) (a) McQuade, D. T.; Pullen, A. E.; Swager, T. M. *Chem. Rev.* **2000**, *100*, 2537. (b) Stott, T. L.; Wolf, M. O. *Coord. Chem. Rev.* **2003**, *246*, 89.

(4) Steffen, W.; Köhler, B.; Altmann, M.; Scherf, U.; Stitzer, K.; zur Loye, H.-C.; Bunz, U. H. F. *Chem. Eur. J.* **2001**, *7*, 117.

(5) (a) MacLachlan, M. J.; Ginzburg, M.; Coombs, N.; Coyle, T. W.; Raju, N. P.; Greedan, J. E.; Ozin, G. A.; Manners, I. *Science* **2000**, *287*, 1460. (b) Park, C.; McAlvin, J. E.; Fraser, C. L.; Thomas, E. L. *Chem. Mater.* **2002**, *14*, 1225.

(6) (a) Berenbaum, A.; Ginzburg-Margau, M.; Coombs, N.; Lough, A. J.; Safa-Sefat, A.; Greedan, J. E.; Ozin, G. A.; Manners, I. *Adv. Mater.* **2003**, *15*, 51. (b) Clendenning, S. B.; Aouba, S.; Rayat, M. S.; Grozea, D.; Sorge, J. B.; Brodersen, P. M.; Sodhi, R. N. S.; Lu, Z.-H.; Yip, C. M.; Freeman, M. R.; Ruda, H. E.; Manners, I. *Adv. Mater.* **2004**, *16*, 215. (c) Clendenning, S. B.; Han, S.; Coombs, N.; Paquet, C.; Rayat, M. S.; Grozea, D.; Brodersen, P. M.; Sodhi, R. N. S.; Yip, C. M.; Lu, Z.-H.; Manners, I. *Adv. Mater.* **2004**, *16*, 291. (d) Lastella, S.; Jung, Y. J.; Yang, H.; Vajtai, R.; Ajayan, P. M.; Ryu, C. Y.; Rider, D. A.; Manners, I. *J. Mater. Chem.* **2004**, *14*, 1791. (e) Chan, W. Y.; Clendenning, S. B.; Berenbaum, A.; Lough, A. J.; Aouba, S.; Ruda, H. E.; Manners, I. *J. Am. Chem. Soc.* **2005**, *127*, 1765.

(7) (a) Massey, J.; Winnik, M. A.; Manners, I.; Chan, V. C. H.; Spatz, J. P.; Ostermann, J. M.; Enchelmaier, R.; Möller, M. *J. Am. Chem. Soc.* **2001**, *123*, 3147. (b) Cheng, J. Y.; Ross, C. A.; Chan, Z.-H.; Thomas, E. L.; Lammertink, R. G. H.; Vancso, G. J. *Adv. Mater.* **2001**, *13*, 1174.

(8) (a) *Inorganic Materials*; Bruce, D. W., O'Hare, D., Eds.; Wiley: New York, 1992. (b) *Extended Linear Chain Compounds*, Miller, J. S., Ed.; Plenum: New York, 1982; Vols. 1–3. (c) Ingham, S. L.; Long, N. J. *Angew. Chem.* **1994**, *106*, 1847; *Angew. Chem., Int. Ed.* **1994**, *33*, 1752. (d) Serrano, J. L. *Adv. Mater.* **1995**, *7*, 348.

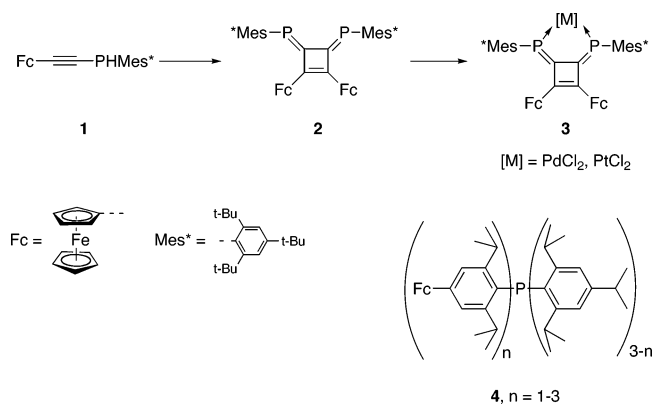
(9) (a) Low, P. J. *Dalton Trans.* **2005**, 2821. (b) Holliday, B. J.; Swager, T. M. *Chem. Commun.* **2005**, 23. (c) Leoni, P.; Marchetti, L.; Mohapatra, S. K.; Ruggeri, G.; Ricci, L. *Organometallics* **2006**, *25*, 4226.

(10) (a) Manners, I. *Chem. Commun.* **1999**, 857. (b) Kingsborough, R. P.; Swager, T. M. *Prog. Inorg. Chem.* **1999**, *48*, 123. (c) Nguyen, P.; Gómez-Elipé, P.; Manners, I. *Chem. Rev.* **1999**, *99*, 1515.

(11) (a) Lehn, J.-M. *Supramolecular Chemistry. Concept and Perspectives*; VCH: Weinheim, 1995.

(12) (a) Schubert, U. S.; Heller, M. *Chem. Eur. J.* **2001**, *7*, 5252. (b) Lahn, B.; Rehahn, M. *Macromol. Symp.* **2001**, *163*, 157.

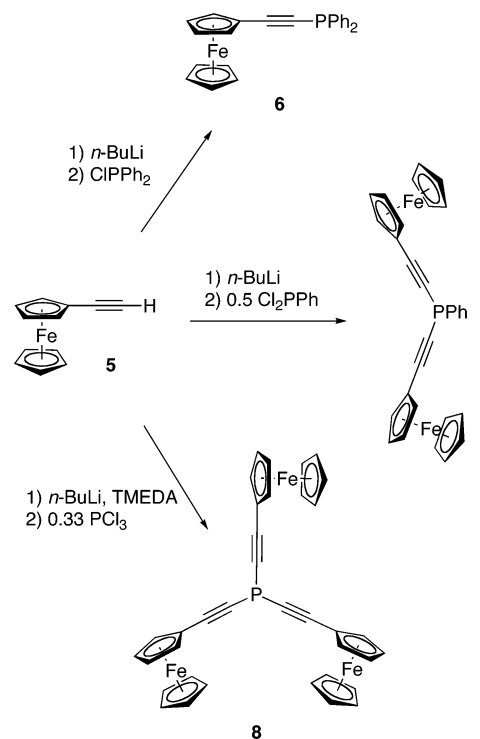
(13) See e.g.: (a) Andres, P. R.; Schubert, U. S. *Adv. Mater.* **2004**, *16*, 1043. (b) Newkome, G. R.; Cho, T. J.; Moorefield C. N.; Mohapatra, P. P.; Godinez, L. A. *Chem. Eur. J.* **2004**, *10*, 1493. (c) Iyer, P. K.; Beck, J. B.; Weder, C.; Rowan, S. J. *Chem. Commun.* **2005**, 319. (d) Maeda, H.; Hasegawa, M.; Hashimoto, T.; Kakimoto, T.; Nishio, S.; Nakanishi, T. *J. Am. Chem. Soc.* **2006**, *128*, 10024.

Scheme 1. Redox-Active, Ferrocenyl-Functionalized Phosphanes^{17,18}


chemistry, the utility of metal–P-donor interactions for the creation of metallopolymers or supramolecular assemblies is relatively unexplored and that the use of value-added spacers is unknown in this context.^{15,16}

As part of our research on organophosphorus and organometallic materials, we have now targeted ferrocenylethynyl-functionalized phosphanes as new, potentially multiredox synthons for the generation of highly metallized materials via metal–P-donor interactions. Yoshifuji and co-workers have recently reported a related building block, **1**, that has been used for the generation of the redox-active, bidentate, low-coordinate P-ligand **2** (Scheme 1).¹⁷ Electrochemical investigations of the corresponding complexes **3** have revealed that the three metal centers within the complexes exhibit strong electronic interactions evident in two reversible {Fe(II) → Fe(III)} and one irreversible {M(II) → M(IV)} oxidation.¹⁷ In 2006, Sasaki and co-workers were able to show that ferrocene-containing, crowded triarylphosphanes **4** also allow strong electronic interactions with multistep reversible redox processes between the attached ferrocene units (Scheme 1).¹⁸ These observations have stimulated us to investigate the (ferrocenylethynyl)phosphane system and determine its potential for molecular electronics.

With the ultimate generation of redox-active supramolecular assemblies and polymers in mind, in the present paper we report our initial studies in this area and describe the synthesis and electronic properties of three novel phosphane ligands as well as corresponding Pd- and Pt-based model complexes to explore the suitability of this structural motif for prospective materials.

Scheme 2. Synthesis of (Ferrocenylethynyl)phosphanes

Results and Discussion

Synthesis of (Ferrocenylethynyl)phosphane Ligands. To verify whether electronic communication between several ferrocene units through a phosphorus center within the same ligand was possible, we synthesized a set of three ligands with increasing number of ferrocenylethynyl moieties (1 → 3). These ligands would provide access to model complexes with two, four, or six ferrocene functionalities, respectively, next to the central transition metal (Pd or Pt). The ethynylene spacer groups of the ligands were anticipated to reduce the steric bulk around the phosphorus center to some extent, but also to promote electronic communication throughout the ligands via π -conjugation. Bearing the design of corresponding bidentate ligands in mind, this structural motif is furthermore expected to suppress potential intramolecular interactions with coordinating transition metal centers due to an unfavorable bite angle in future supramolecular assemblies.^{16b}

Following a known procedure toward the synthesis of phosphinoacetylenes,¹⁹ the mono- and bis-ferrocenylethynyl-functionalized phosphanes **6** and **7** were obtained by reaction of ferrocenylacetylene **5** with *n*-BuLi at -78 °C in THF and subsequent treatment with an appropriate chlorophosphane or dichlorophosphane (Scheme 2). After filtration over neutral alumina, the products were obtained as orange-brown amorphous powders in good isolated yields (**6**: 73%; **7**: 72%). Due to the shielding nature of the electron-rich acetylene unit, their ³¹P NMR signals are considerably high-field shifted, with the bis-ethynyl compound **7** showing a resonance at $\delta^{31}\text{P} = -59.5$ ppm and the mono-ethynyl species **6** at $\delta^{31}\text{P} = -32.8$ ppm. These values compare to those of phenylethynyl analogues, which is also true for the corresponding ¹H and ¹³C NMR spectroscopic data.^{19,20} In the case of the tris(ferrocenylethynyl)phosphane **8**, it should be noted that the synthesis only

(14) (a) Ma, K.; Scheibitz, M.; Scholz, S.; Wagner, M. *J. Organomet. Chem.* **2002**, *652*, 11. (b) Cui, X.; Carapuca, H. M.; Delgado, R.; Drew, M. G. B.; Felix, V. *Dalton Trans.* **2004**, 1743. (c) Dong, T.-Y.; Chang, S.-W.; Lin, S.-F.; Lin, M.-C.; Wen, Y.-S.; Lee, L. *Organometallics* **2006**, *25*, 2018. (d) Köcher, S.; van Klink, G. P. M.; van Koten, G.; Lang, H. *J. Organomet. Chem.* **2006**, *691*, 3319.

(15) (a) Sherlock, S. J.; Cowie, M.; Singleton, E.; de V. Steyn, M. M. *Organometallics* **1988**, *7*, 1663. (b) Wright, M. E.; Lawson, L.; Baker, R. T.; Roe, D. C. *Polyhedron* **1992**, *11*, 323. (c) Puddephatt, R. J. *Coord. Chem. Rev.* **2001**, *216–217*, 313. (d) Paulusse, J. M. J.; Sijbesma, R. P. *Chem. Commun.* **2003**, 1494. (e) Paulusse, J. M. J.; Sijbesma, R. P. *Angew. Chem.* **2004**, *116*, 4560; *Angew. Chem., Int. Ed.* **2004**, *43*, 4460.

(16) (a) Xu, D.; Hong, B. *Angew. Chem., Int. Ed.* **2000**, *39*, 1826. (b) Baumgartner, T.; Huynh, K.; Schleidt, S.; Lough, A. J.; Manners, I. *Chem. Eur. J.* **2002**, *8*, 4622. (c) James, S. L. *Chem. Soc. Rev.* **2003**, *32*, 276. (d) Lin, R.; Yip, J. H. K.; Zhang, K.; Koh, L. L.; Wong, K.-Y.; Ho, K. P. *J. Am. Chem. Soc.* **2004**, *126*, 15852. (e) Martin-Redondo, M. P.; Scoles, L.; Sterenberg, B. T.; Udachin, K. A.; Carty, A. J. *J. Am. Chem. Soc.* **2005**, *127*, 5038. (f) Gianneschi, N. C.; Masar, M. S., III; Mirkin, C. A. *Acc. Chem. Res.* **2005**, *38*, 825.

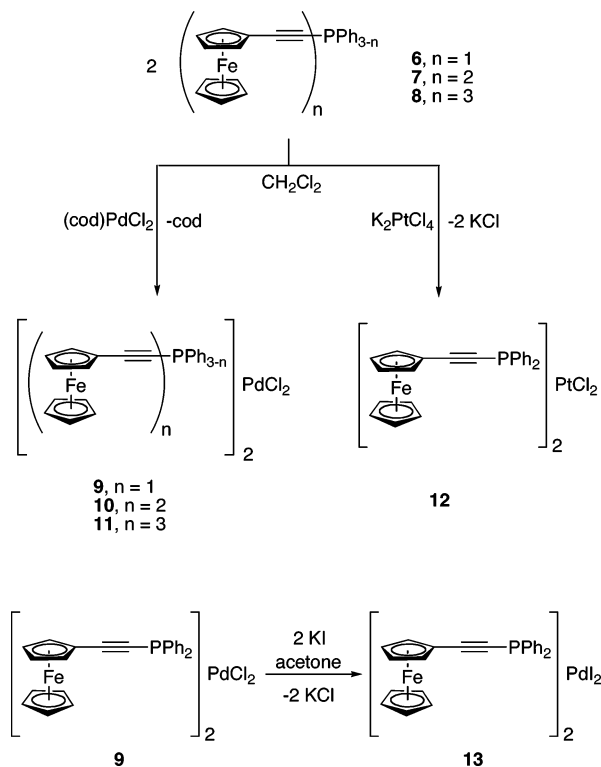
(17) Kawasaki, S.; Nakamura, A.; Toyota, K.; Yoshifuji, M. *Organometallics* **2005**, *24*, 2983.

(18) Sutoh, K.; Sasaki, S.; Yoshifuji, M. *Inorg. Chem.* **2006**, *45*, 992.

(19) Carty, A. J.; Hota, N. K.; Ng, T. W.; Patel, H. A.; O'Connor, T. J. *Can. J. Chem.* **1971**, *49*, 2706.

(20) Hengfeld, A.; Nast, R. *Chem. Ber.* **1983**, *116*, 2035.

Scheme 3. Synthesis of (Ferrocenylethynyl)phosphane Complexes



proceeded to the desired product (isolated yield 57%) when an excess of TMEDA was present in the reaction mixture (Scheme 2). Absence of TMEDA led to a mixture of products that could be identified as mono- and bis(ethynyl) species. This observation was attributed to the steric bulk of the ferrocenylethynyl group, reducing the accessibility of the phosphorus center and only allowing for a trisubstitution with monomeric lithio-acetylenes that are activated by TMEDA. The presence of the three ethynyl groups in **8** leads to a strongly high-field shifted resonance in the ^{31}P NMR spectrum at $\delta = -87.9$ ppm.²⁰

Synthesis and X-ray Crystal Structure Analyses of Pd and Pt Complexes Based on (Ferrocenylethynyl)phosphanes. The synthesis of the PdCl_2 as well as PtCl_2 complexes of the ligands **6–8** was straightforward by following conditions reported in the literature for related complexes.^{16b,21} Complexes **9–12** were obtained via treatment of 2 equiv of the corresponding ligand with 1 equiv of the appropriate complex precursor [$(\text{cod})\text{PdCl}_2$ or K_2PtCl_4] in dichloromethane at room temperature (Scheme 3). The dark red solutions were stirred for 4 h (**9–11**) or 3 days (**12**), respectively, to afford the complexes in very good isolated yields (78–93%). Coordination of the phosphorus centers to the transition metal causes a low-field shift of the ^{31}P NMR resonances ($\Delta\delta = 30\text{--}38$ ppm), now appearing at $\delta^{31}\text{P} = 5.0$ ppm (**9**), $\delta^{31}\text{P} = -24.9$ ppm (**10**), $\delta^{31}\text{P} = -57.8$ ppm (**11**), and $\delta^{31}\text{P} = -17.8$ ppm (**12**). The latter signal also exhibited a $^1\text{J}(\text{P}\text{--}^{195}\text{Pt})$ coupling constant of 3768 Hz, confirming the *cis*-complex geometry, as expected.²² The absence of further resonances in the ^{31}P NMR spectra of **9–12** indicated the formation of only

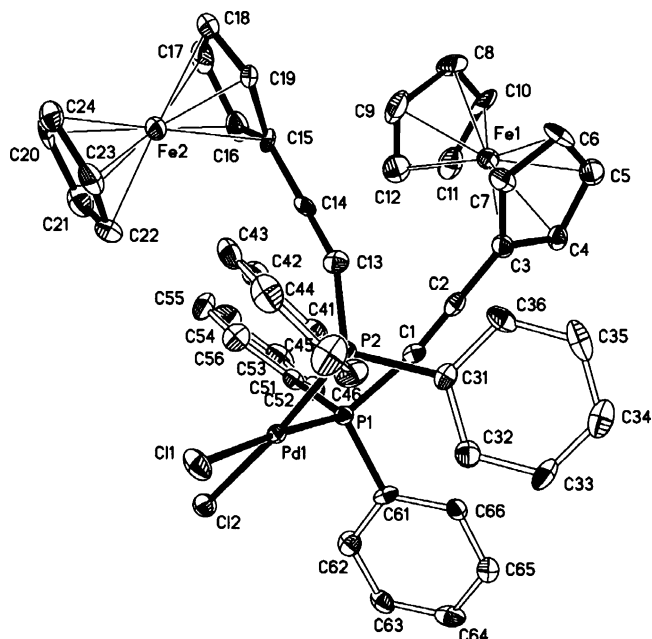


Figure 1. Molecular structure of **9** in the solid state (50% probability level; H atoms omitted for clarity). Selected bonds lengths (Å) and angles (deg): Pd1–P1: 2.2591(16); Pd1–P2: 2.2394(17); P1–C1: 1.758(6); P2–C13: 1.742(6); C1–C2: 1.197(8); C13–C14: 1.206(8); C2–C3: 1.409(9); C14–C15: 1.416(8); C11–Pd1–C12: 90.30(6); P1–Pd1–P2: 93.59(6); P1–Pd1–C11: 175.15(6); P2–Pd1–C12: 174.97(6); Pd1–P1–C1: 117.9(2); Pd1–P2–C13: 108.9(2); P1–C1–C2: 170.7(6); P2–C13–C14: 157.3(6); C1–C2–C3: 179.5(7); C13–C14–C15: 176.1(7).

one complex configuration isomer in each case. The ^1H NMR data of the complexes were comparable to those of the free ligands, with the exception that the *ortho*-H atoms of the phenyl substituents in **9**, **10**, and **12** showed a significant low-field shift.^{16b} The formation of complexes with two phosphane ligands was further corroborated by the respective ^{13}C NMR spectra of the complexes **9–12**, as most of the resonance signals showed either a double doublet or higher order splitting pattern due to coupling with the two different phosphorus centers located at the same and the adjacent ligand. We were also able to obtain suitable single crystals for X-ray crystallographic analyses of **9** and **12** from concentrated solutions ($\text{CH}_2\text{Cl}_2/\text{CHCl}_3$, 1:2) at room temperature that allowed us to confirm the complex geometries. The crystal structure analyses (Figures 1 and 2) revealed that both compounds are *cis*-configured in the solid state and almost isostructural (space group $P2_1/n$). Surprisingly, the ethynyl units show a significant deviation from their genuine linear shape with P1–C1–C2 angles of 170.7(6)° for **9**, 170.3(3)° for **12** and P2–C13–C14 angles of 157.3(6)° for **9**, 156.6(3)° for **12**, which is most likely due to increased steric bulk within the complexes. Furthermore, the two acetylene units in **9** and **12** do not show a coplanar arrangement with the central MCl_2P_2 plane. As observed for related (phenylethynyl)phosphane complexes by Carty et al.²³ and later also by Manners and co-workers,^{16b} the two P–C≡C units exhibit a *cisoid*-arrangement with a torsion angle of 56.7° (**9**) or 56.2° (**12**) between them. However, the torsion angles are significantly smaller than those of the phenylethynyl species (ca. 69°).^{16b,23} The other structural parameters (see Figure 1 and 2) are unexceptional and correspond to those of related compounds.^{16b}

(21) (a) Simpson, R. T.; Carty, A. J. *J. Coord. Chem.* **1973**, 2, 207. (b) Carty, A. J.; Johnson, D. K.; Jacobson, S. E. *J. Am. Chem. Soc.* **1979**, 101, 5612. (c) Carty, A. J.; Efraty, A. *Can. J. Chem.* **1969**, 47, 2573. (d) Forniés, J.; Lalinde, E.; Martín, A.; Moreno, M. T.; Welch, A. J. *J. Chem. Soc. Dalton Trans.* **1995**, 1333.

(22) (a) Power, W. P.; Wasylshen, R. E. *Inorg. Chem.* **1992**, 31, 2176. (b) Lindner, E.; Fawzi, R.; Mayer, H. A.; Eichele, K.; Hiller, W. *Organometallics* **1992**, 11, 1033.

(23) (a) Carty, A. J.; Taylor, N. J.; Johnson, D. K. *J. Am. Chem. Soc.* **1979**, 101, 5422. (b) Johnson, D. K.; Rukachaisirikul, T.; Sun, Y.; Taylor, N. J.; Carty, A. J. *Inorg. Chem.* **1993**, 32, 5544.

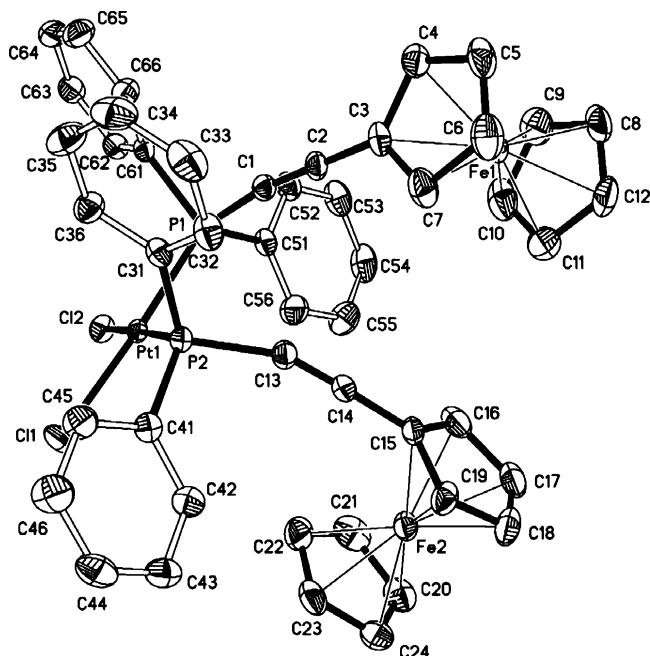


Figure 2. Molecular structure of **12** in the solid state (40% probability level, H atoms omitted for clarity). Selected bonds lengths (Å) and angles (deg): Pt1–P1: 2.2500(9); Pt1–P2: 2.2241(10); P1–C1: 1.755(4); P2–C13: 1.758(4); C1–C2: 1.200(5); C13–C14: 1.200(5); C2–C3: 1.429(5); C14–C15: 1.436(5); C11–Pt1–C12: 88.05(4); P1–Pt1–P2: 94.30(3); P1–Pt1–C11: 174.04(4); P2–Pt1–C12: 176.15(3); Pt1–P1–C1: 117.08(12); Pt1–P2–C13: 109.63(14); P1–C1–C2: 170.3(3); P2–C13–C14: 156.6(3); C1–C2–C3: 178.5(4); C13–C14–C15: 176.8(4).

Carty et al. also established for (phenylethynyl)phosphanes that palladium chloride complexes generally tend to adopt *cis*-configurations, whereas the corresponding palladium iodide complexes are *trans*-configured.^{21,23} To be able to compare potential differences in the electronic properties of the complexes arising from different configurations, we have transformed the PdCl₂ complex **9** into the corresponding PdI₂ species **13** in quantitative yield by treatment of an acetone solution of **9** with potassium iodide at room temperature (Scheme 3, bottom).^{21a} The significantly high-field shifted ³¹P NMR resonance signal of **13** ($\delta = -11.2$ ppm), compared to that of **9** (cf. $\delta^{31}\text{P} = 5.0$ ppm), supported the change of the complex geometry.^{16b} The ¹H and ¹³C NMR spectroscopic data of **13**, on the other hand, were not affected very much by the transformation and relate to those of **9**. The *trans*-geometry was, however, confirmed by an X-ray crystal structure analysis (see Figure 3). Suitable single crystals²⁴ were obtained from a CHCl₃ solution of **13** by slow evaporation of the solvent. The molecular structure of **5** in the solid state exhibits an inversion center about the central Pd atom, leading to a coplanar *transoid*-arrangement of the two P–C≡C units. The fact that the *trans*-configuration of **13** is more favorable than the *cis*-configuration becomes evident in an almost linear acetylene moiety (angle P1–C1–C2: 172.4(12)°), contrasting with the solid-state structures of **9** and **12**. However, the ligands do not show a coplanar arrangement with the central M₂P₂ plane, as already observed for **9** and **12**; for the palladium iodide species **13** the torsion angle amounts to 46.5° (cf. ca. 56° for **9** and **12**), which can be attributed to repulsive interactions between the iodide and the ethynyl group. The other structural parameters are similar to those of **9**, **12**, and related phenylethynyl species (see Figure 3).^{16b,23}

(24) The single crystals of **13** were twinned non-merohedrally, with 880 out of 4634 reflexes affected; BASF for 2nd individual is 0.206.

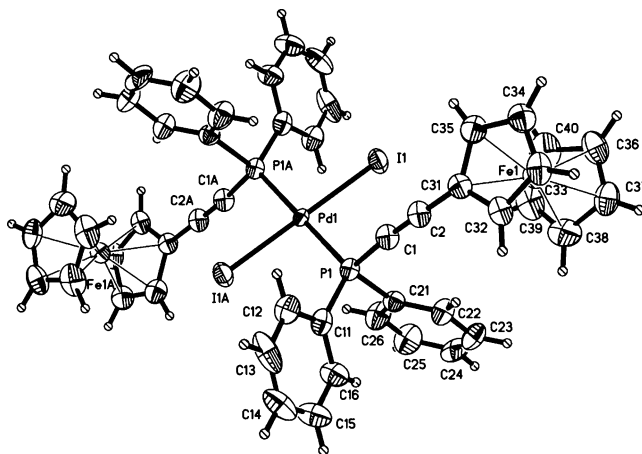


Figure 3. Molecular structure of **13** in the solid state (50% probability level). Selected bonds lengths (Å) and angles (deg): Pd1–P1: 2.314(3); P1–C1: 1.736(12); C1–C2: 1.199(18); C2–C31: 1.420(17); I1–Pd1–I1.A: 180.00(4); P1–Pd1–P1A: 180.0; P1–Pd1–I1: 87.67(8); P1A–Pd1–I1: 92.33(8); Pd1–P1–C1: 114.6(5); P1–C1–C2: 172.4(12); C1–C2–C31: 177.1(13).

We also attempted to synthesize corresponding PtCl₂ complexes based on the bis(ferrocenylethynyl) and tris(ferrocenylethynyl) ligands **7** and **8**. However, the investigation indicated that the steric bulk with the increasing number of ferrocenylethynyl groups is too large to accommodate *cis*-configured complexes. In contrast to their Pd congeners, Pt complexes always adopt this geometry, irrespective of the nature of the ligand of the halogen.^{16b,21,23} Therefore, the ligand **7** was only partially consumed (ca. 50%) to afford the corresponding Pt complex [(FcCC)₂PPh]₂PtCl₂ ($\delta^{31}\text{P} = -40.8$ ppm, $^1J(\text{P}-^{195}\text{Pt}) = 3926$ Hz), even after prolonged reaction times (4 days). Ligand **8** on the other hand did not react at all with the added K₂PtCl₄ and could be recovered completely after 4 days.

Thermal Behavior of the Multi-ferrocene Complexes 10 and 11. The elemental analyses of the complexes **10** and **11**, respectively, always resulted in drastically low carbon values (–7% for **10**; –8% for **11**), indicating the formation of carbides during the combustion process. These observations led us to perform preliminary investigations toward the formation of nanoscale ceramics by means of thermogravimetric analysis (TGA). The results from these studies (Figure 4) further indicated that the two complexes **10** and **11** do form nanocomposites in relatively high yields. Complex **10** gives about 68% ceramic yield, and the major portion of the weight loss can be observed between 300 and 700 °C. The thermal stability of hexaferrocene complex **11**, on the other hand, is significantly greater than that of complex **10**, which can be attributed to the higher metal concentration in **11** compared to **10**. A significant weight loss can be observed only above 550 °C before leveling off at around 950 °C, providing a ceramic yield of ca. 60%. It should be mentioned that both samples recovered after the pyrolysis were also attracted to a bar magnet, which is highly intriguing for potential application in molecular electronics.⁶

Electrochemical Investigations. As mentioned earlier, the ferrocene-containing, crowded triarylphosphanes **4** (Scheme 1) allow strong electronic communication between the attached ferrocene units via the π -conjugated system and the phosphorus center. The same is true for the ferrocenylphosphanes Fc₂PPh and Fc₃P, whose electrochemical behavior was investigated systematically by Barriere, Kirss, and Geiger.²⁵ Both studies

(25) Barriere, F.; Kirss, R. U.; Geiger, W. E. *Organometallics* **2005**, *24*, 48.

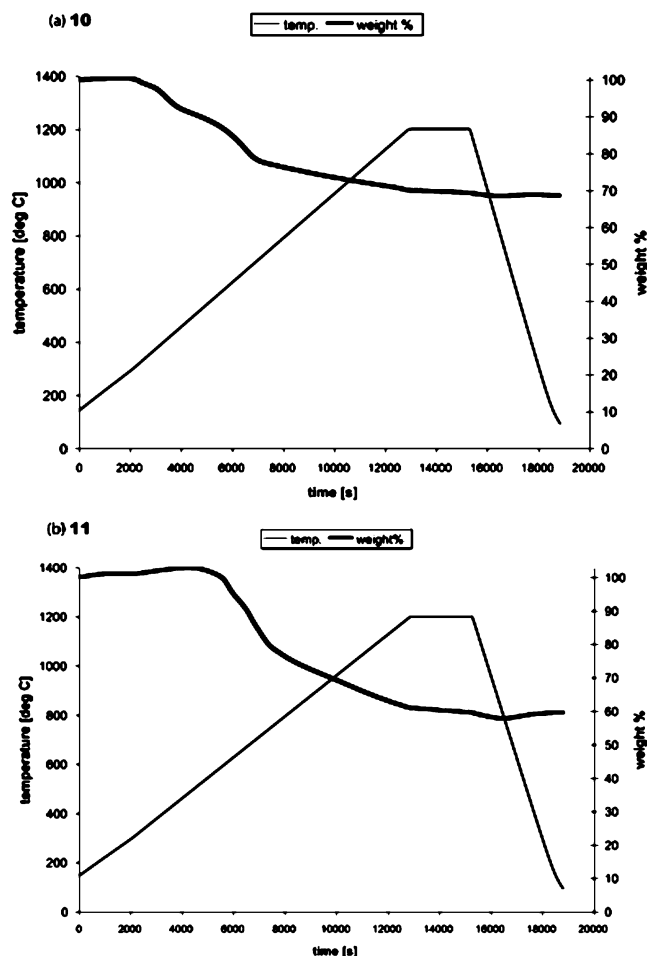


Figure 4. TGA traces and temperature profile of the analyses of complexes **10** (a, top) and **11** (b, bottom).

Table 1. CV Data for Compounds 6–13^a

compound	E_{pc} [V]	E_{pa} [V]
6	0.48	0.59
7	0.50	0.59
8	0.51	0.60
9	0.57	0.69
10	0.55	0.68
11	0.63	0.72
12	0.58	0.70
13	0.54	0.66

^a vs SCE, in CH_2Cl_2 , with 0.1 M $[\text{NBu}_4][\text{PF}_6]$, scan rate 50 mV/s, $T = 293$ K, $E_{1/2}(\text{FcH}/\text{FcH}^+) = 0.4$ V.

have revealed multistep, reversible redox processes for the respective systems that also involve the oxidation of the phosphorus center. In the case of Fc_2PPh and Fc_3P , the first oxidation process seems to involve a species with significant radical cation character at the phosphorus atom. In contrast, oxidation of the phosphorus atom in **4** occurs only *after* the oxidation of the ferrocene units.¹⁸ These observations indicate that different spacer moieties between the ferrocene groups and the central phosphorus atom could lead to a completely different electrochemical behavior. To our surprise, the new ligands **6–8** did indeed show completely different redox properties from the systems reported in the literature. The redox potentials of the ligands **6–8** and the complexes **9–13** are summarized in Table 1. The cyclic voltammograms of **6–8** in CH_2Cl_2 (0.1 mM, $[\text{NBu}_4][\text{PF}_6]$, 50 mV/s, SCE, 293 K) exhibited only one reversible redox wave, respectively, despite the presence of multiple π -conjugated ferrocene units in **7** and **8** (Figure 5). However, the oxidation processes appeared at significantly

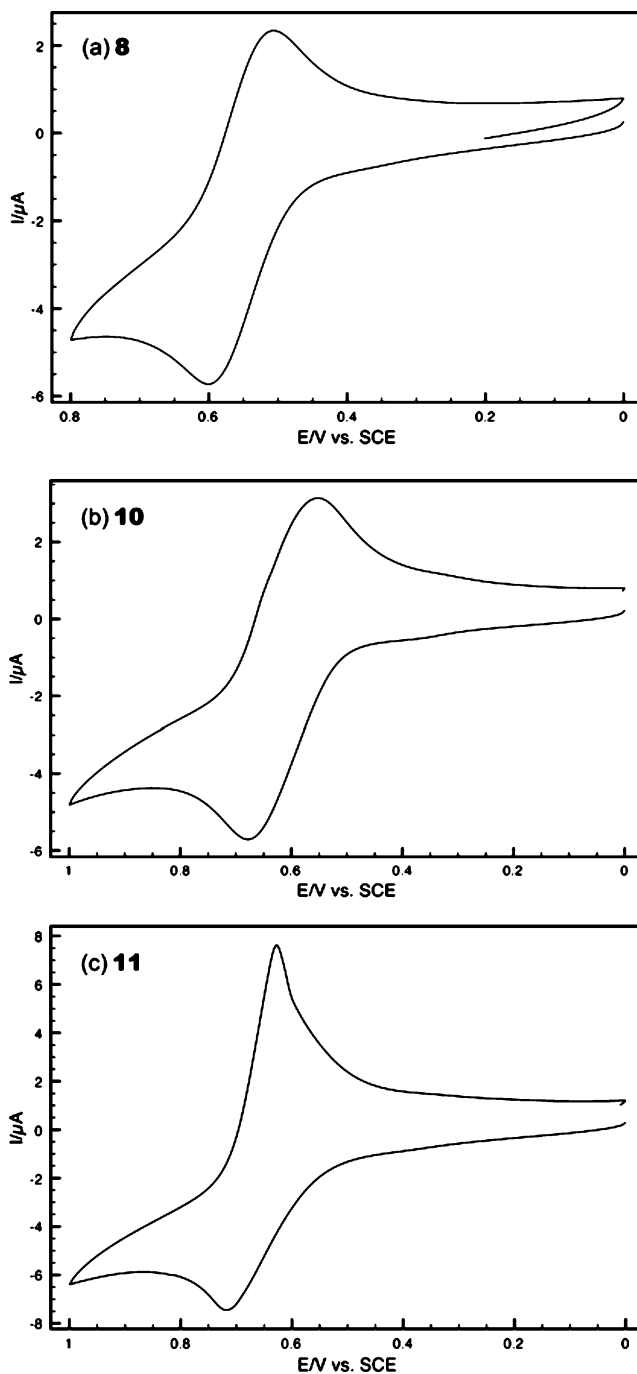


Figure 5. Cyclic voltammograms of **8** (a, top), **10** (b, middle), and **11** (c, bottom) at 293 K. Conditions: Pt disk (0.2 mm²) as working electrode; solutions (ca. 0.1 mM) in CH_2Cl_2 with $[\text{NBu}_4][\text{PF}_6]$ as supporting electrolyte; scan rate 50 mV/s; potentials are referred to the SCE where ferricinium/ferrocene potential is 0.4 V vs SCE.

higher potential than the ferrocene/ferricinium couple (0.4 V vs SCE) at $E_{1/2} = 0.54$ V (**6**), $E_{1/2} = 0.55$ V (**7**), and $E_{1/2} = 0.56$ V (**8**), indicating a potential influence of the substitution pattern at the phosphorus center on the electronic properties of the ligands. The phosphinoacetylene units appear to have an electron-withdrawing effect on the ferrocene moieties, thus leading to increasingly higher oxidation potentials (**6** → **8**) compared to that of native ferrocene. The completely reversible nature of the redox processes suggests the exclusive oxidation of the iron centers, particularly in the presence of $[\text{NBu}_4][\text{PF}_6]$ as supporting electrolyte; under the experimental conditions employed, a radical phosphane species generally would show

some irreversible electrochemical behavior.²⁵ An extension of the observed trend in the redox behavior was found in the corresponding complexes **9**–**11**. The complexes showed single reversible oxidation waves at $E_{1/2} = 0.63$ V (**9**), $E_{1/2} = 0.62$ V (**10**), and $E_{1/2} = 0.68$ V (**11**), also supporting the oxidation of the iron centers, exclusively (Figure 5). The higher potentials in this case could be explained with further decreased electron densities at the ferrocene moieties, caused by the complexation of the phosphorus centers. Considering different complex geometries for complexes **9** and **10/11** could explain the non-linear trend within the observed values. It is very likely that complexes **10** and **11** adopt a *trans*-configuration due to the steric bulk within the ligands. This assumption was further supported by the oxidation potentials of the *cis*-configured Pt complex **12** with $E_{1/2} = 0.64$ V and the *trans*-configured Pd₂ complex **13** at $E_{1/2} = 0.60$ V, indicating that the complex geometry does have an effect on the electrochemical properties of the ferrocene units as well. It should also be mentioned in this context that an oxidation of the transition metal centers in the complexes **9**–**13** was not observed, which is in contrast to the systems **3** investigated by Yoshifuji and co-workers.¹⁷

Conclusion

In conclusion, (ferrocenylethynyl)phosphanes can be synthesized by simple chemical procedures and can easily be transformed into the corresponding Pd or Pt complexes with different complex geometries. The directed syntheses afford highly metalized complexes with up to seven transition metal centers within one molecule. Electrochemical investigations have revealed that the ferrocene moieties do not seem to communicate with each other in either the free ligands or the respective complexes. However, as the redox processes observed are reversible by nature, they can be assigned to exclusively originate from the ferrocene units. The results further indicate that it is possible to generate highly charged, stable materials (up to hexacationic species) that could be suitable for molecular electronics, e.g., as molecular switches. A very intriguing feature with respect to the processability of the materials is the tendency of **10** and **11** to form magnetic ceramics in high yields. A systematic investigation of the new complexes toward materials applications is therefore currently under detailed investigation as well as the synthesis of (ferrocenylethynyl)phosphane-based bidentate ligands to access corresponding supramolecular assemblies.

Experimental Section

General Procedures. All manipulations were carried out under a dry argon atmosphere employing standard Schlenk techniques. Solvents were dried using standard procedures. *n*-BuLi (2.5 M in hexane), K₂PtCl₄, and KI were used as received. Ph₂PCl, PhPCl₂, PCl₃, and TMEDA were freshly distilled prior to use. Ferrocenylacetylene (**5**)²⁶ and (cod)PdCl₂²⁷ were prepared as published. ³¹P{¹H} NMR, ¹H NMR, and ¹³C{¹H} NMR were recorded on a Bruker DRX 400, Varian Mercury 200, or Unity 500 MHz spectrometer. Chemical shifts were referenced to external 85% H₃PO₄ (³¹P) or TMS (¹³C, ¹H). Elemental analyses were performed by the Micro-analytical Laboratory of the RWTH-Aachen University. Thermogravimetric analyses (TGA) were performed using a Setaram Setasys 16/18 instrument under a stream of nitrogen with a heating rate of 2 °C/min. Cyclic voltammetry measurements were performed on a CH-Instruments 630A electrochemical workstation with a Pt

disk (0.2 mm²) as working electrode and solutions (ca. 0.1 mM) in CH₂Cl₂ with [NBu₄]PF₆ as supporting electrolyte. Potentials are referred to the SCE where the ferricinium/ferrocene potential is 0.4 V vs SCE.

Preparation of Ligand 6. To a solution of ferrocenylacetylene (0.92 g, 4.36 mol) in THF (50 mL) was added dropwise *n*-BuLi (1.74 mL, 4.36 mmol) at –78 °C, and the reaction mixture was subsequently warmed to room temperature. After 30 min, the solution was cooled to –78 °C again and Ph₂PCl (0.92 g, 4.36 mmol) was added dropwise. The reaction mixture was allowed to warm, and after 2 h at room temperature the solvent was removed under vacuum. The remaining residue was taken up in dichloromethane and filtered to remove the LiCl. The filtrate was then concentrated and filtered over neutral alumina using pentane as eluent. Evaporation of the solvent afforded **6** as an orange-brown solid. Yield: 1.26 g (73%). ³¹P{¹H} NMR (162.0 MHz, CDCl₃): δ –32.8 ppm. ¹H NMR (500 MHz, CDCl₃): δ 7.65 (m, 4H, *o*-Ph), 7.36 (m, 6H, *p*-Ph, *m*-Ph), 4.53 (pt, ²_J(H,H) = 1.9 Hz, 2H, C₅H₄), 4.25 (pt, ²_J(H,H) = 1.9 Hz, 2H, C₅H₄), 4.22 (s, 5H, Cp) ppm. ¹³C{¹H} NMR (125.0 MHz, CDCl₃): δ 136.8 (d, ¹_J(C,P) = 7.5 Hz, *ipso*-Ph), 132.4 (d, ²_J(C,P) = 21.5 Hz, *o*-Ph), 128.8 (s, *p*-Ph), 128.5 (d, ³_J(C,P) = 8.6 Hz, *m*-Ph), 107.6 (d, *J*(C,P) = 4.8 Hz, C≡C), 81.6 (d, *J*(C,P) = 3.2 Hz, C≡C), 72.0 (s, Cp_{2/5}), 70.0 (s, Cp), 69.2 (s, Cp_{3/4}), 64.2 (s, Cp₁). Anal. Calcd for C₂₉H₁₉FeP: C 73.12; H 4.86. Found: C 73.40; H 5.14. CV: $E_{pc} = 0.48$ V; $E_{pa} = 0.59$ V.

Preparation of Ligand 7. To a solution of ferrocenylacetylene (0.92 g, 4.39 mol) in THF (50 mL) was added dropwise *n*-BuLi (1.76 mL, 4.39 mmol) at –78 °C, and the reaction mixture was subsequently warmed to room temperature. After 30 min, the solution was cooled to –78 °C again, and PhPCl₂ (0.39 g, 2.20 mmol) was added dropwise. The reaction mixture was allowed to warm, and after 2 h at room temperature the solvent was removed under vacuum. The remaining residue was taken up in dichloromethane and filtered to remove the LiCl. The filtrate was then concentrated and filtered over neutral alumina using pentane as eluent. Evaporation of the solvent afforded **7** as a light brown solid. Yield: 0.83 g (72%). ³¹P{¹H} NMR (162.0 MHz, CDCl₃): δ –59.5 ppm. ¹H NMR (500 MHz, CDCl₃): δ 7.77 (m, 2H, *o*-Ph), 7.34 (m, 3H, *p*-Ph, *m*-Ph), 4.45 (pt, ²_J(H,H) = 1.9 Hz, 4H, C₅H₄), 4.16 (pt, ²_J(H,H) = 1.9 Hz, 4H, C₅H₄), 4.16 (s, 10H, Cp) ppm. ¹³C{¹H} NMR (125.0 MHz, CDCl₃): δ 134.4 (br., *ipso*-Ph), 131.5 (d, ²_J(C,P) = 21.4 Hz, *o*-Ph), 129.1 (s, *p*-Ph), 128.7 (d, ³_J(C,P) = 7.5 Hz, *m*-Ph), 106.2 (d, *J*(C,P) = 7.6 Hz, C≡C), 79.4 (br, C≡C), 72.2 (s, Cp₂), 72.1 (s, Cp₅), 70.3 (s, Cp), 69.5 (s, Cp_{3/4}), 63.9 (s, Cp₁). Anal. Calcd for C₃₀H₂₃Fe₂P: C 68.48; H 4.41. Found: C 68.50; H 4.47. CV: $E_{pc} = 0.50$ V; $E_{pa} = 0.59$ V.

Preparation of Ligand 8. To a solution of ferrocenylacetylene (1.01 g, 4.81 mol) in THF (50 mL) and TMEDA (2.18 mL, 14.42 mL) was added dropwise *n*-BuLi (1.94 mL, 4.81 mmol) at –78 °C, and the reaction mixture was subsequently warmed to room temperature. After 30 min, the solution was cooled to –78 °C again, and PCl₃ (0.22 g, 1.60 mmol) was added dropwise. The reaction mixture was allowed to warm, and after 3 h at room temperature the solvent was removed under vacuum. The remaining residue was taken up in dichloromethane and filtered to remove the LiCl. The filtrate was subsequently filtered over neutral alumina using dichloromethane as eluent. Evaporation of the solvent afforded **8** as an orange-brown solid. Yield: 0.60 g (57%). ³¹P{¹H} NMR (162.0 MHz, CDCl₃): δ –87.9 ppm. ¹H NMR (400 MHz, CD₂-Cl₂): δ 4.48 (pt, ²_J(H,H) = 1.9 Hz, 6H, C₅H₄), 4.21 (pt, ²_J(H,H) = 1.9 Hz, 6H, C₅H₄), 4.20 (s, 15H, Cp) ppm. ¹³C{¹H} NMR (100.0 MHz, CD₂Cl₂): δ 105.8 (d, *J*(C,P) = 12.1 Hz, C≡C), 76.7 (d, *J*(C,P) = 8.7 Hz, C≡C), 72.5 (s, Cp₂), 72.4 (s, Cp₅), 70.6 (s, Cp), 70.0 (s, Cp_{3/4}), 63.5 (s, Cp₁). Anal. Calcd for C₃₆H₂₇Fe₃P: C 65.70; H 4.14. Found: C 65.34; H 4.22. CV: $E_{pc} = 0.51$ V; $E_{pa} = 0.60$ V.

General Procedure for the Synthesis of the PdCl₂ Complexes **9–**11**.** Two equivalents of the corresponding ligand (2 mmol; **6**:

(26) Doisneau, G.; Balavoine, G.; Fillebeen-Khan, T. J. *Organomet. Chem.* **1992**, *425*, 113.

(27) Drew, D.; Doyle, J. R. *Inorg. Synth.* **1972**, *13*, 52.

Table 2. Crystallographic Data for **9**, **12**, and **13**

	9	12	13
formula	C ₄₈ H ₃₈ Cl ₂ Fe ₂ P ₂ Pd	C ₄₈ H ₃₈ Cl ₂ Fe ₂ P ₂ Pt	C ₄₈ H ₃₈ Fe ₂ I ₂ P ₂ Pd
<i>M_r</i>	965.72	1054.41	1148.62
<i>T</i> /K	120(2)	200(2)	228(2)
cryst syst	monoclinic	monoclinic	triclinic
space group	<i>P</i> 2 ₁ / <i>n</i> (no. 14)	<i>P</i> 2 ₁ / <i>n</i> (no. 14)	<i>P</i> $\bar{1}$ (no. 2)
<i>a</i> /Å	10.8183(8)	10.895(2)	7.601(3)
<i>b</i> /Å	21.3720(15)	21.539(4)	12.040(2)
<i>c</i> /Å	17.4369(13)	17.514(3)	13.0166(17)
α /deg	90	90	107.208(13)
β /deg	93.297(3)	93.625(3)	101.176(19)
γ /deg	90	90	102.58(2)
<i>V</i> /Å ³	4024.9(5)	4101.6(14)	1067.0(5)
<i>Z</i> , <i>D_c</i> /Mg cm ⁻³	4, 1.594	4, 1.708	1, 1.787
<i>F</i> (000)	1952	2080	560
μ (Mo K α)/mm ⁻¹	1.400	4.343	2.642
θ range for data collection	1.51 to 26.10	1.50 to 30.04	2.03 to 26.96
no. of reflns collected/unique (<i>R</i> _{int})	47 441/7984 (0.1251)	42 887/11 399 (0.0515)	9272/4636 (0.0386)
no. of data/restraints/params	7984/0/496	11 399/0/496	4636/0/250
final <i>R</i> indices [<i>I</i> > 2 σ (<i>I</i>)]	<i>R</i> ₁ = 0.0704, <i>wR</i> ₂ = 0.1216	<i>R</i> ₁ = 0.0302, <i>wR</i> ₂ = 0.0641	<i>R</i> ₁ = 0.0845, <i>wR</i> ₂ = 0.2790
<i>R</i> indices (all data)	<i>R</i> ₁ = 0.0952, <i>wR</i> ₂ = 0.1302	<i>R</i> ₁ = 0.0521, <i>wR</i> ₂ = 0.0743	<i>R</i> ₁ = 0.0931, <i>wR</i> ₂ = 0.2841
GOF on <i>F</i> ²	1.164	1.092	1.109
largest diff peak and hole/e Å ³	0.624 and -0.869	1.046 and -1.000	5.969 and -1.571

0.79 g; **7**: 1.04 g; **8**: 1.31 g) were dissolved in dichloromethane (30 mL), and 1 equiv of (cod)PdCl₂ (0.28 g, 1 mmol) was added at room temperature. The dark red-brown suspensions were stirred for 4 h at room temperature, and the solvent was subsequently removed under vacuum. The resulting solids were treated with pentane to remove residual cyclooctadiene and recrystallized from dichloromethane/chloroform (1:2) to afford complexes **9**–**11** as air-stable, dark red crystals (**9**) or glassy solids (**10**, **11**). Yields: 93%, 0.90 g (**9**); 80%, 0.98 g (**10**); 78%, 1.16 g (**11**).

Complex 9. ³¹P{¹H} NMR (80.9 MHz, CDCl₃): δ 5.0 ppm. ¹H NMR (400 MHz, CD₂Cl₂): δ 7.89 (dd, ³*J*(H,P) = 13.4 Hz, ³*J*(H,H) = 7.4 Hz, 8H, *o*-Ph), 7.54 (t br., ³*J*(H,H) = 7.4 Hz, 4H, *p*-Ph), 7.45 (t br., ³*J*(H,H) = 7.7 Hz, 8H, *m*-Ph), 4.27 (pt, ^{2/4}*J*(H,H) = 2.0 Hz, 4H, C₅H₄), 4.20 (pt, ^{2/4}*J*(H,H) = 2.0 Hz, 4H, C₅H₄), 4.06 (s, 10H, Cp) ppm. ¹³C{¹H} NMR (100.0 MHz, CD₂Cl₂): δ 134.0 (pt, *J*(C,P) = 6.2 Hz, *o*-Ph), 131.7 (s, *p*-Ph), 130.3 (dd, ¹*J*(C,P) = 66.8 Hz, ³*J*(C,P) = 2.6 Hz, *ipso*-Ph), 128.8 (pt, *J*(C,P) = 5.9 Hz, *m*-Ph), 113.6 (m, *J*(C,P) = 9.2 Hz, C \equiv C), 76.2 (dd, *J*(C,P) = 111.9 Hz, *J*(C,P) = 8.1 Hz, C \equiv C), 72.6 (s, Cp_{2/5}), 70.6 (s, Cp_{3/4}), 70.5 (s, Cp), 61.3 (s, Cp₁). Anal. Calcd for C₄₈H₃₈Cl₂Fe₂P₂Pd: C 59.69; H 3.97. Found: C 59.85; H 4.06. CV: *E*_{pc} = 0.57 V; *E*_{pa} = 0.69 V.

Complex 10. ³¹P{¹H} NMR (162.0 MHz, CD₂Cl₂): δ -24.9 ppm. ¹H NMR (400 MHz, CD₂Cl₂): δ 8.21 (dd, ³*J*(H,P) = 15.9 Hz, ³*J*(H,H) = 8.0 Hz, 4H, *o*-Ph), 7.57 (m, 6H, *p*, *m*-Ph), 4.27 (d pt, *J*(H,P) = 2.5 Hz, ^{2/4}*J*(H,H) = 1.8 Hz, 8H, C₅H₄), 4.31 (pt, ^{2/4}*J*(H,H) = 1.8 Hz, 8H, C₅H₄), 4.22 (s, 20H, Cp) ppm. ¹³C{¹H} NMR (100.0 MHz, CD₂Cl₂): δ 133.2 (pt, *J*(C,P) = 7.8 Hz, *o*-Ph), 132.1 (s, *p*-Ph), 130.0 (dd, ¹*J*(C,P) = 80.6 Hz, ³*J*(C,P) = 2.4 Hz, *ipso*-Ph), 129.1 (pt, *J*(C,P) = 7.4 Hz, *m*-Ph), 111.6 (m, *J*(C,P) = 11.7 Hz, C \equiv C), 74.4 (dd, *J*(C,P) = 133.5 Hz, *J*(C,P) = 3.8 Hz, C \equiv C), 72.8 (d, *J*(C,P) = 4.3 Hz, Cp_{2/5}), 70.8 (s, Cp), 70.8 (d, *J*(C,P) = 3.0 Hz, Cp_{3/4}), 61.4 (pt, ^{3/5}*J*(C,P) = 1.3 Hz, Cp₁). Anal. Calcd for C₆₀H₆₄-Cl₂Fe₄P₂Pd: C 58.60; H 3.77. Found: C 51.69; H 3.57. CV: *E*_{pc} = 0.55 V; *E*_{pa} = 0.68 V.

Complex 11. ³¹P{¹H} NMR (162.0 MHz, CDCl₃): δ -57.8 ppm. ¹H NMR (400 MHz, CD₂Cl₂): δ 4.55 (pt, ^{2/4}*J*(H,H) = 1.6 Hz, 12H, C₅H₄), 4.23 (br, 42H, C₅H₄/Cp) ppm. ¹³C{¹H} NMR (100.0 MHz, CD₂Cl₂): δ 109.1 (m, *J*(C,P) = 15.6 Hz, C \equiv C), 72.4 (dd, *J*(C,P) = 154.8 Hz, *J*(C,P) = 2.6 Hz, C \equiv C), 72.6 (s, Cp_{2/5}), 70.7 (s, Cp), 70.2 (s, Cp_{3/4}), 61.1 (pt, ^{3/5}*J*(C,P) = 1.7 Hz, Cp₁). Anal. Calcd for C₇₂H₅₄Cl₂Fe₆P₂Pd: C 57.90; H 3.64. Found: C 49.46; H 3.51. CV: *E*_{pc} = 0.63 V; *E*_{pa} = 0.72 V.

Preparation of 12. Two equivalents of ligand **6** (0.79 g, 2 mmol) were dissolved in dichloromethane (30 mL), and 1 equiv of K₂-PtCl₄ (0.42 g, 1 mmol) was added at room temperature. The red-

brown suspension was stirred for 3 days at room temperature and filtered subsequently to remove the generated KCl. The solvent was then removed under vacuum and the residue washed a couple of times with cold chloroform to afford **12** as an air-stable, bright red solid. Yield: 0.90 g (85%). Single crystals, suitable for X-ray crystallography were obtained from a concentrated solution (CH₂-Cl₂/CHCl₃, 1:2) at room temperature. ³¹P{¹H} NMR (162.0 MHz, CD₂Cl₂): δ -11.2 (*J*(P,Pt) = 3768 Hz) ppm. ¹H NMR (400 MHz, CD₂Cl₂): δ 7.86 (dd, ³*J*(H,P) = 13.4 Hz, ³*J*(H,H) = 8.2 Hz, 8H, *o*-Ph), 7.54 (t m, ³*J*(H,H) = 7.5 Hz, 4H, *p*-Ph), 7.45 (t m, ³*J*(H,H) = 7.4 Hz, 8H, *m*-Ph), 4.25 (pt, ^{2/4}*J*(H,H) = 2.0 Hz, 4H, C₅H₄), 4.18 (pt, ^{2/4}*J*(H,H) = 2.0 Hz, 4H, C₅H₄), 4.05 (s, 10H, Cp) ppm. ¹³C{¹H} NMR (100.0 MHz, CDCl₃): δ 134.0 (pt, *J*(C,P) = 6.9 Hz, *o*-Ph), 131.7 (s, *p*-Ph), 129.8 (dd, ¹*J*(C,P) = 78.5 Hz, ³*J*(C,P) = 2.2 Hz, *ipso*-Ph), 128.8 (pt, *J*(C,P) = 6.5 Hz, *m*-Ph), 113.6 (m, *J*(C,P) = 10.0 Hz, C \equiv C), 75.3 (dd, *J*(C,P) = 127.5 Hz, *J*(C,P) = 4.8 Hz, C \equiv C), 72.6 (s, Cp_{2/5}), 70.5 (s, Cp_{3/4}), 70.4 (s, Cp), 61.3 (s, Cp₁). Anal. Calcd for C₄₈H₃₈Cl₂Fe₂P₂Pt: C 54.68; H 3.63. Found: C 54.06; H 3.67. CV: *E*_{pc} = 0.58 V; *E*_{pa} = 0.70 V.

Preparation of Complex 13. To a solution of complex **9** (0.49 g, 0.5 mmol) in acetone (20 mL) was added KI (0.17 g, 1 mmol) at room temperature. The reaction mixture was then stirred for 30 min and the solvent removed under vacuum subsequently. The residue was taken up in dichloromethane and filtered, and the filtrate was evaporated to dryness. Recrystallization from chloroform afforded **13** as air-stable dark orange-red single crystals. Yield: 1.02 g (89%). ³¹P{¹H} NMR (80.9 MHz, CDCl₃): δ -17.8 ppm. ¹H NMR (400 MHz, CDCl₃): δ 7.73 (m, 8H, *o*-Ph), 7.39 (m br, 4H, *p*-Ph), 7.35 (m br, 8H, *m*-Ph), 4.55 (pt, ^{2/4}*J*(H,H) = 1.8 Hz, 4H, C₅H₄), 4.21 (s, 12H, C₅H₄/Cp) ppm. ¹³C{¹H} NMR (100.0 MHz, CDCl₃): δ 133.5 (pt, *J*(C,P) = 6.2 Hz, *o*-Ph), 129.6 (s, *p*-Ph), 127.5 (pt, *J*(C,P) = 6.6 Hz, *ipso*-Ph), 127.0 (pt, *J*(C,P) = 5.8 Hz, *m*-Ph), 112.1 (pt, *J*(C,P) = 8.7 Hz, C \equiv C), 79.1 (pt, *J*(C,P) = 54.2 Hz, C \equiv C), 71.4 (s, Cp_{2/5}), 69.3 (s, Cp), 68.7 (s, Cp_{3/4}), 61.4 (s, Cp₁). Anal. Calcd for C₄₈H₃₈I₂Fe₂P₂Pd: C 50.19; H 3.33. Found: C 49.94; H 3.37. CV: *E*_{pc} = 0.54 V; *E*_{pa} = 0.66 V.

X-ray Structure Determination. For complexes **9** and **12**, data were collected on a Bruker SMART D8 goniometer with an APEX CCD detector at 120 K (**9**) or 200 K (**12**), respectively, and for complex **13** on an Enraf-Nonius CAD4 at 228 K, using Mo K α radiation (λ = 0.71073 Å, graphite monochromator). The SADABS²⁸ method of absorption correction was applied in all cases.

(28) Sheldrick, G. M. *SADABS*, Program for Empirical Absorption Correction of Area Detector Data; University of Göttingen: Germany, 1996.

The structures were solved by direct methods (SHELXTL)²⁹ and refined on F^2 by full-matrix least-squares techniques. All non-hydrogen atoms were refined anisotropically. Hydrogen atoms were placed geometrically and refined using a riding model. Crystal data and details of data collection and structure refinements are given in Table 2.

Acknowledgment. The authors thank Prof. Dr. Jun Okuda for his generous support of this work. Financial support of the Fonds der Chemischen Industrie (FCI), BMBF, and the Deutsche

(29) Sheldrick, G. M. *SHELXTL*, Version 5.1; Bruker AXS Inc.: Madison, WI, 1998.

Forschungsgemeinschaft (DFG) is gratefully acknowledged. We thank Prof. Dr. U. Englert for the X-ray data collection and helpful discussions, Prof. Dr. U. Kölle for his assistance with the cyclic voltammetry, and D. Müller and Y. Dienes for their assistance with the TGA measurements. T.B. thanks the University of Calgary for start-up funding.

Supporting Information Available: Complete tables of crystal data collections and unit-cell parameters, positional parameters, and bond distances and angles for **9**, **12**, and **13**. This material is available free of charge via the Internet at <http://pubs.acs.org>.

OM0606892